



Article

Altered Dynamic Functional Connectivity of Cuneus in Schizophrenia Patients: A Resting-State fMRI Study

Charles Okanda Nyatega^{1,2,*} , Li Qiang³, Mohammed Jajere Adamu³ , Ayesha Younis³
and Halima Bello Kawuwa⁴

¹ School of Electrical and Information Engineering, Tianjin University, Tianjin 300072, China

² Department of Electronics and Telecommunication Engineering, Mbeya University of Science and Technology, Mbeya P.O. Box 131, Tanzania

³ School of Microelectronics, Tianjin University, Tianjin 300072, China; liqiang@tju.edu.cn (L.Q.); mainajajere@tju.edu.cn (M.J.A.); ayesha@tju.edu.cn (A.Y.)

⁴ School of Precision Instrument and Opto-Electronics Engineering, Tianjin University, Tianjin 300072, China; halima@tju.edu.cn

* Correspondence: ncharlz@tju.edu.cn



Citation: Nyatega, C.O.; Qiang, L.; Adamu, M.J.; Younis, A.; Kawuwa, H.B. Altered Dynamic Functional Connectivity of Cuneus in Schizophrenia Patients: A Resting-State fMRI Study. *Appl. Sci.* **2021**, *11*, 11392. <https://doi.org/10.3390/app112311392>

Academic Editors:
Marianna Semprini and Jing Jin

Received: 17 August 2021

Accepted: 25 November 2021

Published: 1 December 2021

Publisher's Note: MDPI stays neutral with regard to jurisdictional claims in published maps and institutional affiliations.



Copyright: © 2021 by the authors. Licensee MDPI, Basel, Switzerland. This article is an open access article distributed under the terms and conditions of the Creative Commons Attribution (CC BY) license (<https://creativecommons.org/licenses/by/4.0/>).

Abstract: Objective: Schizophrenia (SZ) is a functional mental condition that has a significant impact on patients' social lives. As a result, accurate diagnosis of SZ has attracted researchers' interest. Based on previous research, resting-state functional magnetic resonance imaging (rsfMRI) reported neural alterations in SZ. In this study, we attempted to investigate if dynamic functional connectivity (dFC) could reveal changes in temporal interactions between SZ patients and healthy controls (HC) beyond static functional connectivity (sFC) in the cuneus, using the publicly available COBRE dataset. Methods: Sliding windows were applied to 72 SZ patients' and 74 healthy controls' (HC) rsfMRI data to generate temporal correlation maps and, finally, evaluate mean strength (dFC-Str), variability (dFC-SD and ALFF) in each window, and the dwelling time. The difference in functional connectivity (FC) of the cuneus between two groups was compared using a two-sample *t*-test. Results: Our findings demonstrated decreased mean strength connectivity between the cuneus and calcarine, the cuneus and lingual gyrus, and between the cuneus and middle temporal gyrus (TPomid) in subjects with SZ. Moreover, no difference was detected in variability (standard deviation and the amplitude of low-frequency fluctuation), the dwelling times of all states, or static functional connectivity (sFC) between the groups. Conclusions: Our verdict suggest that dynamic functional connectivity analyses may play crucial roles in unveiling abnormal patterns that would be obscured in static functional connectivity, providing promising impetus for understanding schizophrenia disease.

Keywords: schizophrenia; static functional connectivity; dynamic functional connectivity; sliding window; cuneus; variability; mean strength; standard deviation; rsfMRI; COBRE

1. Introduction

Schizophrenia (SZ) is a mental condition in which individuals experience hallucinations [1], delusions, and profoundly disorganized thinking and behavior as a result of their erroneous interpretation of reality. Positive symptoms such as hallucinations, delusions, and flight of ideas are common in SZ patients, as are negative symptoms such as apathy, emotionlessness, lack of social functioning, and cognitive symptoms such as difficulties concentrating and paying attention, as well as memory deficits [2]. Literature suggests that a person's risk of developing the illness is increased by a mix of physical, genetic, psychological, and environmental variables. A stressful or emotional life experience may precipitate a psychotic episode in some persons who are predisposed to SZ. Approximately half of SZ patients have a history of drug abuse disorders [3], and nearly all of them smoke [4]. An Omega-3 polyunsaturated fatty acids (PUFAs) dietary imbalance could aggravate its course while also raising the risk of metabolic complications [5]. Despite the availability of

effective pharmacological treatments for HC, up to 50% of patients experience poor illness outcomes [6,7]. Many possible outcome factors have been revealed in group-level research, including disease-course characteristics, treatment adherence and response, comorbidity, and cognitive impairments [8]. It is yet unclear which of these features should be used for prediction, or whether findings at the group-level can be utilized to make meaningful predictions for individuals with SZ [9].

We can now use neuroimaging technologies, such as MRI, computed tomography, and positron emission tomography (PET), to research brain structure and function, thanks to advances in neuroimaging technology. Through the measurement of the blood oxygenation level-dependent (BOLD) signal, functional MRI (fMRI) can provide information about the properties of FC—that is, collections of brain regions that are coactivated to support shared functions—during task or at rest (i.e., in the absence of stimuli) [10–12]. Different task-based studies of functional magnetic resonance imaging (fMRI) [13,14] unveiled changes between SZ and HC groups, but they have faced the challenge of difficulty in interpretation since subjects perform different scanning tasks [15]. Resting-state fMRI (rsfMRI) examines behavioral characteristics such as personality, psychological states, temperament traits, sustained attention, and creative capacity, and cognitive abilities such as working memory and motor function [16–19]. The majority of fMRI studies that have looked into FC in SZ have used static functional connectivity (sFC) methods, which involve averaging FC across the scanning time. These methods are based on the premise that the FC between brain regions does not change significantly during the course of the scanning session, which lasts about 5–15 min. However, in light of mounting evidence suggesting significant changes in fMRI FC across time, this assumption does not appear to be correct [20,21]. As a result, current rsfMRI research has increasingly focused on time-varying FC or dynamic FC (dFC) [22,23]. The goal of these studies is to find connection patterns that can be seen across individuals at different times during the scanning period [24,25]. When it comes to categorizing SZ patients, dFC has been demonstrated to outperform sFC measurements [26,27].

Although there is substantial evidence that the brain FC of patients with SZ is abnormal [28–31] the differences in functional connectivity observed in SZ are inconsistent across different studies. For instance, some works have revealed increased FC in the default mode region in patients with SZ [32], and increased connectivity involving default mode region nodes and cortical and subcortical domain nodes [33], whilst reduced or mixed FC was seen between cortical regions and default mode regions [34]. Although this increased/decreased FC could be due to differences in disease symptoms or subtypes, we believe that part of the heterogeneity is due to comparisons made using a static connectivity measure of FC that represents an average across different dynamic modes of brain activity during an unconstrained resting state [15].

To discover the intrinsic neural changes in visual-related diseases, FC analysis has been successfully used between the primary visual cortex and patients with amblyopia [35], glaucoma [36], and retinal vein occlusion [37]. Our study focuses on the cuneus as it plays a role in both primary and secondary visual processing such as spatial frequency, orientation, motion, direction, and speed. It is located in the medial occipital gyri, part of the occipital lobe, corresponding to Broadmann area 17, which receives input from the contralateral superior retina corresponding to the lower visual field [38]. The cuneus connects to activation in the precuneus of the parietal lobe via the dorsal stream, which functionally is associated with spatial awareness and representations of object locations [39]. Activation in the ventral stream connects the cuneus to a smaller volume of activation in the inferior temporal cortex of the temporal lobe, which is functionally involved with object recognition [40] such as circles against the pattern of squares [41] and blue and red color perception [42]. One study associated greater inhibitory control among patients with Bipolar Disorder I with greater cuneus volume [43], and increased activity in the cuneus when compared with controls was found in compulsive gamblers [44] in another study. Patients with localized brain lesions are more likely to have associated with damage to the cuneus [38]. Visual functions (e.g., movement perception) are also affected by damage to

more anterior parts of the cuneus, though usually for higher-level operations such as object perception and spatial processing, such as attention [45].

Different analysis tools have been used to describe brain FC using rsfMRI data, including seed-based [11,38], independent component analysis (ICA) [15,46–48], principal component analysis (PCA) [49], clustering [50,51], fisher discriminant dictionary learning (FDDL) [52], centrality [53], multivariate pattern analysis (MVPA) [54,55], and graph theory [56,57]. In this study, we used seed-based analysis, in which the connectivity patterns are based on a selected seed region of interest (ROI). The advantage of this method is that the results are focused on particular ROIs and, hence, could be easier to understand in relation to neuropathology [58].

With rsfMRI data of 72 SZ patients and 74 HC groups from the COBRE dataset, sFC and dFC were used to analyze the whole brain in both groups, and the dynamic characteristics (standard deviation (SD) and mean strength (Str)) were used to estimate the dFC. We used the proposed seed-based FC method to obtain the FC between the cuneus and other brain regions and compare whether sFC and dFC might provide factual information by identifying dFC indicators in order to understand SZ neural mechanisms better.

2. Materials and Methods

2.1. Participants

Data used in this study were from COBRE [59], consisting of 72 SZ patients (fourteen females and fifty-eight males) and 74 HCs (twenty-three females and fifty-one males). Participants were screened and ruled out if they had a history of neurological illness, mental retardation, extreme head trauma resulting in more than 5 min of loss of consciousness, or history of drug abuse or dependence during the previous 12 months. Diagnostic information was collected using the Structured Clinical Interview used for DSM Disorders (SCID) [59]. The inclusion was of men and women of 37.0 ± 12.78 years of age. Collected T1-weighted (MPRAGE) image parameters were: voxel size = $1 \text{ mm} \times 1 \text{ mm} \times 1 \text{ mm}$ flip angle = 7° , echo time (TE) = 1.64, 3.5, 5.36, 7.22, 9.08, repetition time (TR) = 2530, field of view (FoV) = $256 \text{ mm} \times 256 \text{ mm}$, inversion time (TI) = 900 ms, thickness = 176 mm, matrix = $256 \times 256 \times 176$. Functional MRI data were gathered with: TR/TE = 2 s/29 ms, 33 slices, voxel size: $3 \times 3 \times 4 \text{ mm}^3$, matrix = 64×64 , and 150 time points. All participants were asked to remain relaxed and keep their eyes open during the scan.

2.2. Data Preprocessing

Data were pre-processed using Data Processing Assistant for Resting-State fMRI (DPARSF, V5.0, <http://rfmri.org> [60], accessed on 23 November 2021, Statistical Parametric Mapping (SPM V12) [61], and MATLAB V2018b [62] Toolboxes.

The steps for data preprocessing were as follows: one subject was discarded because of having too-few time points in image data (67 instead of 150). For the rest of subjects, we removed the first five volumes, leaving 145 volumes; corrected slice-timing and realigned images; manually reoriented the T1 and functional images; co-registered T1 images into functional images then segmented images to gray matter (GM), white matter (WM), and cerebrospinal fluid (CSF); nuisance covariates were regressed (including Friston 24 head motion parameters [63] and white matter and cerebrospinal fluid signals), functional images were then normalized into MNI space DARTEL Method [64] and resliced to $3.0 \times 3.0 \times 3.0 \text{ mm}^3$; spatial smoothing of normalized images was performed at 6 mm FWHM; band-pass filtering images at 0.01–0.08 Hz as it was found that resting-state signals are consistent low-frequency fluctuations in this range [65]. To address head motion in fMRI, image volumes with mean framewise displacement FD (Jenkinson) $> 0.5 \text{ mm}$ were scrubbed to reduce its effect using cubic spline interpolation [66,67]. Subjects were not excluded as they did not exceed the head transition $< 3 \text{ mm}$, rotation $< 3^\circ$ [68].

2.3. Regions of Interest Definition and Network

To identify differences in rsFC between SZ and HC groups, regions obtained from the automated anatomical labelling template (AAL) [69] were applied to determine the FC based on the region of interest (ROI). Except the cerebellum [70], the 90 ROIs of AAL were divided into prefrontal regions, other regions of frontal lobe, parietal regions, occipital regions, temporal regions, and subcortical regions. Finally, mean time courses from all 90 ROIs were extracted to calculate functional connectivity.

2.4. Static Resting-State Functional Connectivity

With the remaining 145-image volumes, we estimated the Pearson's correlation coefficient of Fisher's z transformation between each pair of the mean time course in 90 ROIs, to enhance the normality of correlation distribution [70] and for the construction of the static rsFC brain network.

2.5. Dynamic Resting-State Functional Connectivity

The sliding window method [50] was applied, implementing a window size at 30 TRs (60 s) being that 30 s to 60 s is considered good enough [15,50,71]. We selected a sliding temporal window length of 30 TRs (60 s) to 145 data length (290 s). Rectangular sliding windows unconvolved with a Gaussian kernel were then used to capture sharper transitions that could be undetected in a tapered window [72]. By sliding the window by the 2 s step size 1 TR, 116 temporal windows ($145 - 30 + 1$) were generated. Finally, 116 Fisher's z-transformed Pearson's correlation maps (90×90 matrix size, for each window) for each subject were obtained as the dynamic functional connectivity maps (Figure 1).

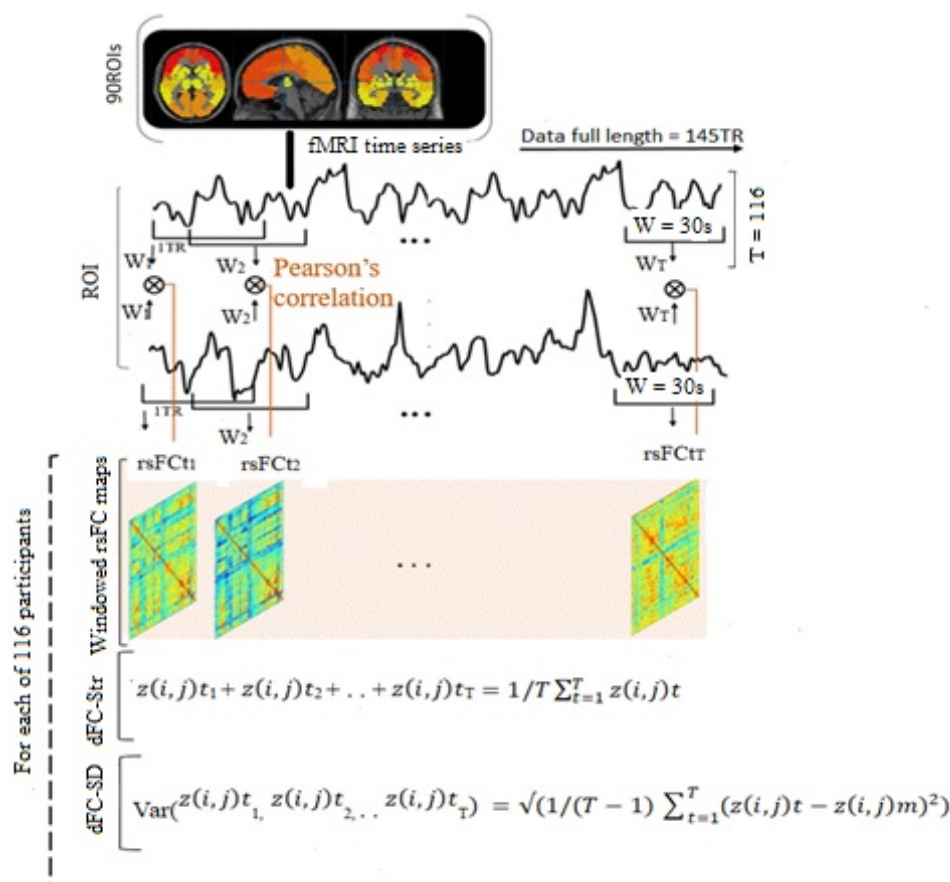


Figure 1. Dynamic network analysis flow-chart. A total of 90 ROIs times series from AAL template were extracted from fMRI data (145 TR), from which a rectangular sliding window ($W = 30$ s) was used to generate dynamic rsFC maps.

2.6. Measurements of the Dynamic Characteristics

Mean strength and temporal variability (standard deviation and the amplitude of low-frequency fluctuation (ALFF)) were measured in order to demonstrate the dynamic characteristics, as follows:

$$dFC - Str(i, j) = \frac{1}{T \sum_{t=1}^T z(i, j)_t} \quad (1)$$

$$dFC - SD(i, j) = \sqrt{(1/(T-1) \sum_{t=1}^T (z(i, j)_t - z(i, j)_m)^2)} \quad (2)$$

where: $z(i, j)_t$ represents ROI i and j FC value at window t , $z(i, j)_m$; mean/average of $z(i, j)_t$ over the total of T windows [73], dFC-Str; strength and dFC-SD as temporal variability.

For the ALFF analysis, it was carried out using DPABI. The power spectrum was produced by transforming the filtered time series of each voxel into the frequency domain using a Fast Fourier Transform. We calculated ALFF for each voxel by taking the square root of the signal at 0.01–0.08 Hz [74]. The ALFF of each voxel was further divided by the global mean of ALFF values for each participant within the default brain mask from the DPABI, with background and other non-brain tissue signals discarded, for uniformity and to limit the influence of individual variance in ALFF values. This resulted in a standardized ALFF map for the entire brain.

2.7. Characterization of dFC States' Property

We examined the mean dwelling time (MDT), which measures the amount of time an individual spends in a specific state, to see if SZ had any effect on the features of transient states [24,75].

2.8. Statistical Analyses

We applied two-sample t -tests to test whether the mean strength (dFC-Str) and temporal variability (dFC-SD and ALFF) within each temporal windowed connectivity map present any significant differences between SZ and HC groups. False Discovery Rate (FDR)-corrected activations with $p < 0.05$ [76,77] were conducted, with confounding variables such as age, gender, IQ, and handed-ness (Table 1) as covariates in the GRETNA toolbox [78]. Permutation tests ($p < 0.05$) were also used to evaluate the differences between groups in state properties (MDT).

Table 1. Participant demographics.

	Schizophrenia (n = 72)	Healthy Controls (n = 74)	p-Value
Age (years)	38.17 ± 13.89	35.82 ± 11.58	0.270 ¹
Sex (Female/Male)	14/58	23/51	0.106 ²
Handed-ness			
Right/Left/Both	60/10/2	71/1/2	0.106 ²
IQ	(n = 68)	(n = 67)	
Verbal	97.88 ± 16.73	106.79 ± 11.16	<0.001 ¹
Performance	102.68 ± 16.64	114.03 ± 12.32	<0.001 ¹
Sum	99.59 ± 16.86	108.33 ± 11.83	<0.001 ¹
PANSS (n = 72)			
Positive scale	14.96 ± 4.83		
Negative scale	14.53 ± 4.83		
General	29.22 ± 8.34		
Education (years)	12.99 ± 1.84	13.52 ± 1.75	0.089 ¹
Illness duration (years, n = 71)	16.03 ± 12.41		

¹ Two-sample t -test. ² Chi-square test. Data are shown in mean ± SD.

3. Results

3.1. Participants' Demographic and Neuropsychological Evaluation

Table 1 shows subjects' clinical information, in which no significant difference was seen between age, sex, handed-ness, and education years of the two groups ($p > 0.05$) by two-sample t -tests. However, significant differences were seen in IQ ($p < 0.05$) using two-sample t -tests. The PANSS scales were reported in the patients' group and the primary diagnosis information for the SZ patient group and the HC group are presented in Table 2. Other information available in COBRE INDI Additional data in Supplementary Materials.

Table 2. Primary diagnosis information for schizophrenia patients and healthy controls.

Diagnosis (DSM Code)	Number
<i>Patients:</i>	
Dementia of the Alzheimer's type, with late onset, with delirium (290.3)	1
Disorganized type (295.1)	3
Catatonic type (295.2)	1
Paranoid type (295.3)	41
Residual type (295.6)	12
Bipolar type I (295.7)	1
Depresses type (295.7)	1
Schizoaffective Disorder type (295.7)	5
Undifferentiated type (295.9)	5
Bipolar Disorder type I, Most Recent Episode Mixed, In Full Remission (296.4)	1
Unspecified type schizophrenia chronic state (295.92)	1
<i>Healthy Controls:</i>	
Major Depressive Disorder, Single Episode, In Partial Remission (296.26)	1
Depressive Disorder type, Not Otherwise Specified (311)	1
Other Healthy Controls (none)	72

DSM, Diagnostic and Statistical Manual of Mental Disorders.

3.2. Static Functional Connectivity

No significant difference ($p > 0.05$) was apparent in static $rsFC$ between schizophrenia patients and healthy controls (Table 3 at 290 s), suggesting that static $rsFC$ might be insensitive in capturing neural functional abnormalities underlying schizophrenia.

Table 3. The group difference of dFC-Str (four connections) for different window sizes (Movie S1).

Time/Windows Connections	44 s (22 TRs)	60 s (30 TRs)	100 s (50 TRs)	150 s (75 TRs)	290 s (145 TRs)
CUN.L-CAL.R	6.17×10^{-6}	5.68×10^{-6}	6.13×10^{-6}	6.33×10^{-6}	-
CUN.R-CAL.R	1.53×10^{-5}	1.56×10^{-5}	4.60×10^{-5}	-	-
LING.R-CUN.R	1.89×10^{-5}	1.98×10^{-5}	2.40×10^{-5}	2.12×10^{-5}	-
TPOmid.R-CUN.R	4.72×10^{-5}	4.89×10^{-5}	2.58×10^{-5}	2.80×10^{-5}	-

Table shows p -values of group differences of dFC-Str. Numbers represent significant difference after FDR correction. L, left; R, right; Mid, Middle.

3.3. Dynamic Functional Connectivity

With resting-state fMRI, the SZ patient group demonstrated a significantly decreased mean strength across time windows (dFC-Str) between the left cuneus (CUN.L) and right calcarine (CAL.R) ($p = 0.00000568$), between the right cuneus (CUN.R) and the right calcarine (CAL.R) ($p = 0.0000156$), between the right lingual gyrus (LING.R) and right cuneus (CUN.R) ($p = 0.0000198$), and between the right-middle temporal gyrus (TPOmid.R) and right cuneus (CUN.R) ($p = 0.0000489$) with t values -4.79 , -4.54 , -4.48 , and -4.25 , respectively. (Figures 2 and 3, Table 3, Movie S1).

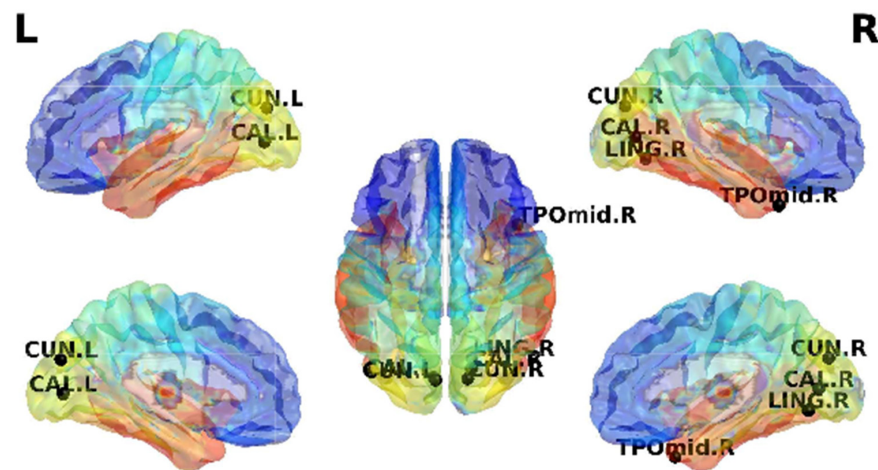


Figure 2. The group significant difference using GLM, FDR correction ($q < 0.05$). CUN, Cuneus; CAL, Calcarine; LING, lingual gyrus; TPOmid, middle temporal gyrus; L, Left; R, Right.

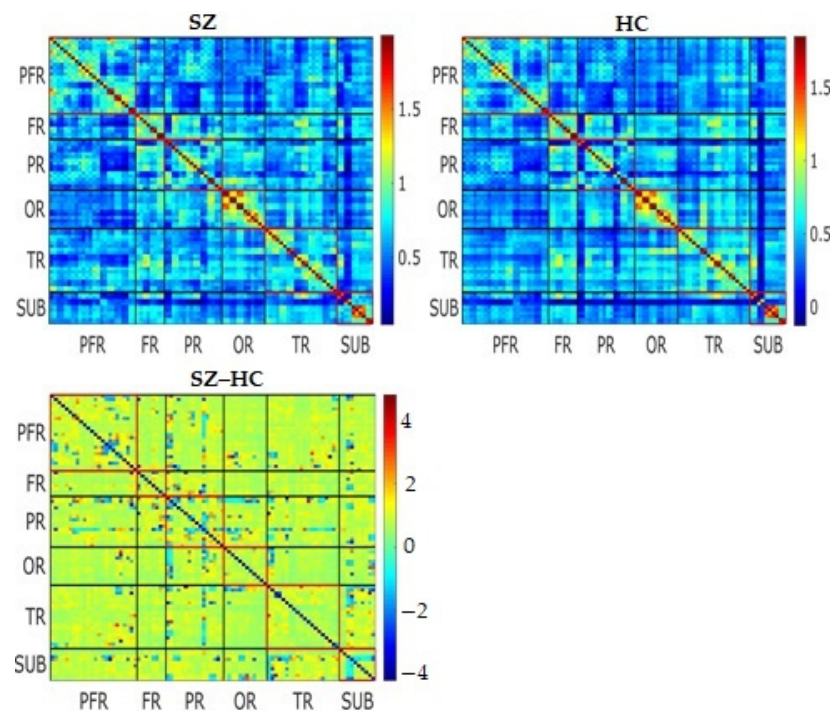


Figure 3. The mean strength (dFC-Str) matrices of SZ and HC groups where **SZ** is for schizophrenia patients, **HC** for healthy controls and **SZ-HC** is the group difference in the average dynamic rsFC that survived FDR thresholding. Values are plotted as $-\log_{10}(p\text{-value}) \times \text{sign}(t\text{-statistic})$. The lines partition the rsFC maps into six subcategories (i.e., prefrontal (PFR), other frontal (FR), parietal (PR), occipital (OR), temporal (TR), and subcortical regions (SUB)).

In contrast to mean strength between the groups, variability (dFC-SD and ALFF) within all temporal windows did not present significant differences ($p > 0.05$) between the SZ patient group and the HC group. Furthermore, there were no significant differences in the dwelling times of all states between the two groups. The significant level here was FDR-corrected $p < 0.05$.

4. Discussion

This is one of the few dFC studies of schizophrenia based on the COBRE public dataset [79–83]. In this study, we investigated differences in functional connectivity (FC) dynamics at rest between schizophrenia (SZ) patients and healthy controls (HC). Sliding

windows were used to construct dynamic resting-state functional connectivity maps whose windowed cuneus-connectivity properties were assessed. We also explored the group differences in large time-scale connectivity (static perspective), which were computed as correlations of fMRI time series over the full range of scanning time. We found that, while there were no significant differences in static functional connectivity (sFC), mean strength (dFC-Str) analyses presented SZ patients with decreased cuneus-connectivity findings that could not be identified in static analyses. However, the variability of cuneus connectivity did not demonstrate any significant difference between the groups in all temporal correlation-windows.

The cuneus is delimited by the parieto-occipital sulcus and the calcarine sulcus in the occipital lobe, known for its role in both primary and secondary visual processing. With respect to decreased functional connectivity, fairly similar findings to our observations were reported in previous studies such as decreased gray-matter volumes in the cuneus and lingual gyrus as compared to healthy participants [84,85]. Another study illustrated that when glaucoma patients were compared to healthy people, the functional connectivity of the cuneus decreased [36,86]. The cuneus also indicated substantial reduction in brain neural homogeneity in people with acute open-globe injury [87] and retinal detachment [88] in another study. Some other studies emphasize that smaller volumes of gray matter in the right cuneus [89] and lower activity in the cuneus and precuneus [90] were associated with suicide attempters. Tohid and colleagues found reduced activation in the right cuneus and fusiform gyrus during episodic memory retrieval in SZ patients compared with HCs [91]. In a first-episode psychosis study, patients with poor insight had decreased gray matter volume in the cuneus and medial gyrus of the right occipital lobe as compared to those with good insight [92]. Together, these findings suggest that patients with schizophrenia are characterized by altered cuneus connectivity in large scale brain networks.

Previous investigations, on the other hand, were unable to identify reduced connectivity in the cuneus, but did find it in the occipital lobe. For example, Glahn et al. (2008) found a reduced gray-matter density in SZ patients relative to HCs [93], lower global connectivity [94], and decreased connectivity strength [95]. The previous study by Phillips and colleagues revealed reduced external white matter fractional anisotropy, especially in bilateral occipital lobes, in SZ patients compared to their relatives [96]. Hallucination was also associated with a reduced volume of the occipital lobe in SZ patients [97], reduction in the overall volume of occipital lobe in SZ [97–99], lower white-matter volume in first-episode patients, and decreased activation in fusiform gyrus [100–102]. No cuneus-connectivity attenuation was reported by the authors in all these studies. One reason could be the limitations of analysis techniques or because alterations in brain activity linked to illnesses are not always supported by large-scale evidence. Rather, they are visible across a small time-scale of seconds, necessitating short time-scale investigations to capture those deficit patterns.

In our study, SZ patients exhibited decreased cuneus mean strength connectivity (dFC-Str) in several brain areas, such as the left cuneus and right calcarine, the right cuneus and right calcarine, the right cuneus and right lingual gyrus, and between the right cuneus and right-middle temporal gyrus. These changes were all observed in dFC and not in sFC, this may be because some brain disorders need short-time-scale analyses in order to capture subtle deficits. Previous and current rsfMRI researches on SZ have increasingly focused on dFC [1,22,23], especially in specific time intervals (windows) [15,23,103–107]. Our results are in accordance with Damaraju et al. in SZ and Nguyen et al. in Bipolar Disorder studies, who demonstrated how dynamic FC has more predictive accuracy than static FC [15,108]. We also observed similar connections in different time. The evidence in Table 3 shows how the connections were lost in bigger window sizes (Table 3 at 75 TR) and at full-length (145 TR). Together, these findings point to the conclusion that information that is likely to be lost in static FC (bigger window sizes approaching to full-length) can be trapped in the dynamic FC.

Although we only found a decrease in cuneus connectivity in this study, previous research has found that SZ can also cause an increase in cuneus connectivity. Notably, increased dynamic ReHo was also discovered in the superior temporal gyrus, postcentral gyrus, thalamus, middle cingulum cortex, and cuneus in SZ patients [106]. Other regions have also been linked to an increased functional connectivity in SZ illnesses, such as an increased global-brain functional connectivity in the left superior frontal gyrus [109].

Even though the majority of SZ studies have emphasized the decreased FC patterns, the lack of increased connection patterns in these studies and our study could be linked to the type of SZ patients regarding the stage of illness and medication [110]. The brain compensatory mechanism's inability to recruit more resources to retain, maintain, or restore cognitive functioning, or in response to cognitive demands, can be viewed as the main indication of decreased connectivity in SZ. Since it has long been assumed that SZ is a spectrum of diseases caused by several pathophysiological processes rather than a single disease [111], other factors such as diverse samples and different preprocessing approaches could also lead to this inconsistency.

Even though the cuneus is believed to be associated with cognitive functions such as behavior engagement [112], working memory [113], and cognitive control [43]. It is thought to be largely engaged in visual processing. The cuneus, in particular, appears to be involved in detecting changes in ocular position as a result of spontaneous eye movements [114]. Impairments in smooth-pursuit eye movements have been repeatedly recorded, especially in SZ patients [115]. These studies reveal that SZ patients, or those who are at risk of developing the condition, may have problems monitoring their own eye movements and this could be because of reduced connectivity in the cuneus. Evidenced by previous works, the SZ decreased connectivity in visual areas could also be because those affected typically perform worse in visual motion [116] and visual contrast [117]. Whether the cuneus anatomical abnormalities seen in the SZ subjects in this study are also related to abnormal eye tracking is a topic worthy of future discussion.

Limitations

Our study, however, presented some limitations; first, 41 subjects (more than half of SZ) were of Paranoid type, suggesting that it is unclear whether the observed results were of all SZ patients or were influenced by the large paranoid-type data (57%). Second, patients with schizophrenia may be using a variety of antipsychotic medications, which may influence their cognitive functions. A previous study revealed that SZ patients showed synchronized brain activity and decreased integration function across brain networks after undergoing six-week treatment with second-generation antipsychotic medications [118]. These antipsychotic medications may also affect their brain activities. For example, olanzapine treatment increased default mode network (DMN) connectivity in patients with SZ [119]. Hence, attention should be paid while interpreting our results. Third, although we did not achieve statistical significance in variability, it is possible that a better-designed study could provide more definite results. Fourth, the lack of neuropsychological tests for SZ and HC may also limit the study since the data used in this study were obtained online (COBRE), resulting in no correlation analysis between altered rsFC and neuropsychological evaluation in both groups. Thus, intergroup difference in neuropsychological evaluation also remains unknown. Fifth, the authors of this work acknowledge that the sliding window technique has a number of drawbacks [25,120,121], such as that multiple parameters must be specified including window function, length, and step size, but due to a shortage of ground truth in resting-state fMRI data, the ideal settings are still uncertain. We confirm that our work, just like the vast majority of resting-state-dFC studies have employed this technique, mainly due to its simplicity [71]. Lastly, our biggest challenge was to obtain the dataset, and the main reason was the COVID-19 pandemic, which limited us only to use publicly available dataset.

5. Conclusions

In this study, we used seed-based method to obtain the FC between the cuneus and other brain regions in individuals with schizophrenia. Results revealed that patients with SZ indicated decreased mean strength connectivity in short-time-based analysis (dynamic) in the cuneus, relative to their matched healthy control, while presenting no significant differences in variability and full-time (static) sense. This suggests that strong insights in understanding brain deficits underlying schizophrenia can be provided by dynamic-connectivity analyses of the cuneus. This hypothesis will need to be investigated further, utilizing various structural, functional, and metabolic methodologies. To address the suppressing effect associated with the sliding windows, the authors of this work are looking forward to use windows with a flattened spectrum within the bandwidth such as modulated rectangular (mRect) [122] in our future studies.

Supplementary Materials: The following are available online at <https://www.mdpi.com/article/10.3390/app112311392/s1>, Table S1: COBRE INDI Additional data, Movie S1: The group significant difference.

Author Contributions: Conceptualization, C.O.N. and L.Q.; software, C.O.N.; validation, L.Q.; formal analysis, C.O.N., M.J.A. and A.Y.; investigation, A.Y. and H.B.K.; resources, L.Q. and C.O.N.; data curation, M.J.A. and H.B.K.; writing—original draft preparation and methodology, C.O.N. and M.J.A.; writing—review and editing, C.O.N.; visualization, A.Y. and H.B.K.; supervision and project administration, L.Q. All authors have read and agreed to the published version of the manuscript.

Funding: This research received no external funding.

Informed Consent Statement: Not applicable.

Data Availability Statement: Data used in this study are available at the COBRE publicly archived datasets at http://fcon_1000.projects.nitrc.org/indi/retro/cobre.html (accessed on 23 November 2021).

Acknowledgments: The authors thank all individuals who served as research participants.

Conflicts of Interest: The authors declare no conflict of interest.

References

1. Weber, S.; Johnsen, E.; Kroken, R.A.; Løberg, E.-M.; Kandilarova, S.; Stoyanov, D.; Kompus, K.; Hugdahl, K. Dynamic Functional Connectivity Patterns in Schizophrenia and the Relationship With Hallucinations. *Front. Psychiatry* **2020**, *11*, 227. [CrossRef]
2. Tanaka, M.; Tóth, F.; Polyák, H.; Szabó, Á.; Mándi, Y.; Vécsei, L. Immune Influencers in Action: Metabolites and Enzymes of the Tryptophan-Kynurenine Metabolic Pathway. *Biomedicines* **2021**, *9*, 734. [CrossRef]
3. Volkow, N.D. Substance Use Disorders in Schizophrenia—Clinical Implications of Comorbidity. *Schizophr. Bull.* **2009**, *35*, 469–472. [CrossRef] [PubMed]
4. Goff, D.C.; Henderson, D.C.; Amico, E. Cigarette smoking in schizophrenia: Relationship to psychopathology and medication side effects. *Am. J. Psychiatry* **1992**, *149*, 1189–1194. [CrossRef] [PubMed]
5. Rog, J.; Błazewicz, A.; Juchnowicz, D.; Ludwiczuk, A.; Stelmach, E.; Koziół, M.; Karakula, M.; Niziński, P.; Karakula-Juchnowicz, H. The Role of GPR120 Receptor in Essential Fatty Acids Metabolism in Schizophrenia. *Biomedicines* **2020**, *8*, 243. [CrossRef] [PubMed]
6. Freyhan, F.A. Course and outcome of schizophrenia. *Am. J. Psychiatry* **2006**, *112*, 161–169. [CrossRef] [PubMed]
7. Häfner, H.; der Heiden, W.A. The course of schizophrenia in the light of modern follow-up studies: The ABC and WHO studies. *Eur. Arch. Psychiatry Clin. Neurosci.* **1999**, *249*, S14–S26. [CrossRef] [PubMed]
8. Tsang, H.W.H.; Leung, A.Y.; Chung, R.C.K.; Bell, M.; Cheung, W.-M. Review on vocational predictors: A systematic review of predictors of vocational outcomes among individuals with schizophrenia: An update since 1998. *Aust. N. Z. J. Psychiatry* **2010**, *44*, 495–504. [CrossRef] [PubMed]
9. Komatsu, H.; Watanabe, E.; Fukuchi, M. Psychiatric Neural Networks and Precision Therapeutics by Machine Learning. *Biomedicines* **2021**, *9*, 403. [CrossRef]
10. Kim, J.; Kim, Y.-K. Crosstalk between Depression and Dementia with Resting-State fMRI Studies and Its Relationship with Cognitive Functioning. *Biomedicines* **2021**, *9*, 82. [CrossRef] [PubMed]
11. Biswal, B.; Yetkin, F.Z.; Haughton, V.M.; Hyde, J.S. Functional connectivity in the motor cortex of resting human brain using echo-planar MRI. *Magn. Reson. Med.* **1995**, *34*, 537–541. [CrossRef]

12. Smitha, K.A.; Akhil Raja, K.; Arun, K.M.; Rajesh, P.G.; Thomas, B.; Kapilamoorthy, T.R.; Kesavadas, C. Resting state fMRI: A review on methods in resting state connectivity analysis and resting state networks. *Neuroradiol. J.* **2017**, *30*, 305–317. [[CrossRef](#)] [[PubMed](#)]
13. Mathalon, D.H.; Ford, J.M. Divergent approaches converge on frontal lobe dysfunction in schizophrenia. *Am. J. Psychiatry* **2008**, *165*, 944–948. [[CrossRef](#)] [[PubMed](#)]
14. Mazoyer, B.; Zago, L.; Mellet, E.; Bricogne, S.; Etard, O.; Houdé, O.; Crivello, F.; Joliot, M.; Petit, L.; Tzourio-Mazoyer, N. Cortical networks for working memory and executive functions sustain the conscious resting state in man. *Brain Res. Bull.* **2001**, *54*, 287–298. [[CrossRef](#)]
15. Damaraju, E.; Allen, E.A.; Belger, A.; Ford, J.M.; McEwen, S.; Mathalon, D.H.; Mueller, B.A.; Pearlson, G.D.; Potkin, S.G.; Preda, A.; et al. Dynamic functional connectivity analysis reveals transient states of dysconnectivity in schizophrenia. *NeuroImage Clin.* **2014**, *5*, 298–308. [[CrossRef](#)] [[PubMed](#)]
16. Balogh, L.; Tanaka, M.; Török, N.; Vécsei, L.; Taguchi, S. Crosstalk between Existential Phenomenological Psychotherapy and Neurological Sciences in Mood and Anxiety Disorders. *Biomedicines* **2021**, *9*, 340. [[CrossRef](#)] [[PubMed](#)]
17. Jiang, R.; Calhoun, V.D.; Zuo, N.; Lin, D.; Li, J.; Fan, L.; Qi, S.; Sun, H.; Fu, Z.; Song, M.; et al. Connectome-based individualized prediction of temperament trait scores. *Neuroimage* **2018**, *183*, 366–374. [[CrossRef](#)] [[PubMed](#)]
18. Hsu, W.-T.; Rosenberg, M.D.; Scheinost, D.; Constable, R.T.; Chun, M.M. Resting-state functional connectivity predicts neuroticism and extraversion in novel individuals. *Soc. Cogn. Affect. Neurosci.* **2018**, *13*, 224–232. [[CrossRef](#)]
19. Rosenberg, M.D.; Finn, E.S.; Scheinost, D.; Papademetris, X.; Shen, X.; Constable, R.T.; Chun, M.M. A neuromarker of sustained attention from whole-brain functional connectivity. *Nat. Neurosci.* **2015**, *19*, 165–171. [[CrossRef](#)]
20. Chang, C.; Glover, G.H. Time-frequency dynamics of resting-state brain connectivity measured with fMRI. *Neuroimage* **2010**, *50*, 81–98. [[CrossRef](#)]
21. Hutchison, R.M.; Womelsdorf, T.; Gati, J.S.; Everling, S.; Menon, R.S. Resting-state networks show dynamic functional connectivity in awake humans and anesthetized macaques. *Hum. Brain Mapp.* **2013**, *34*, 2154–2177. [[CrossRef](#)] [[PubMed](#)]
22. Du, Y.; Fryer, S.L.; Fu, Z.; Lin, D.; Sui, J.; Chen, J.; Damaraju, E.; Mennigen, E.; Stuart, B.; Loewy, R.L.; et al. Dynamic functional connectivity impairments in early schizophrenia and clinical high-risk for psychosis. *Neuroimage* **2018**, *180*, 632–645. [[CrossRef](#)]
23. He, H.; Luo, C.; He, C.; He, M.; Du, J.; Biswal, B.B.; Yao, D.; Yao, G.; Duan, M. Altered Spatial Organization of Dynamic Functional Network Associates With Deficient Sensory and Perceptual Network in Schizophrenia. *Front. Psychiatry* **2021**, *12*, 687580. [[CrossRef](#)] [[PubMed](#)]
24. Calhoun, V.D.; Miller, R.; Pearlson, G.; County, B. The Chronnectome: Time-Varying Connectivity Networks as the Next Frontier in fMRI Data Discovery. *Neuron* **2014**, *84*, 262–274. [[CrossRef](#)]
25. Hutchison, R.M.; Womelsdorf, T.; Allen, E.A.; Bandettini, P.A.; Calhoun, V.D.; Corbetta, M.; Della Penna, S.; Duyn, J.H.; Glover, G.H.; Gonzalez-Castillo, J.; et al. Dynamic functional connectivity: Promise, issues, and interpretations. *Neuroimage* **2013**, *80*, 360–378. [[CrossRef](#)] [[PubMed](#)]
26. Rashid, B.; Arbabshirani, M.; Damaraju, E.; Cetin, M.; Miller, R.; Pearson, G.; Calhoun, V.D. Classification of schizophrenia and bipolar patients using static and dynamic resting-state fMRI brain connectivity. *Neuroimage* **2016**, *134*, 645–657. [[CrossRef](#)] [[PubMed](#)]
27. Cetin, M.S.; Houck, J.M.; Rashid, B.; Agacoglu, O.; Stephen, J.M.; Sui, J.; Canive, J.; Mayer, A.; Aine, C.; Bustillo, J.R.; et al. Multimodal Classification of Schizophrenia Patients with MEG and fMRI Data Using Static and Dynamic Connectivity Measures. *Front. Neurosci.* **2016**, *10*, 466. [[CrossRef](#)] [[PubMed](#)]
28. Breakspear, M.; Terry, J.R.; Friston, K.J.; Harris, A.W.F.; Williams, L.M.; Brown, K.; Brennan, J.; Gordon, E. A disturbance of nonlinear interdependence in scalp EEG of subjects with first episode schizophrenia. *Neuroimage* **2003**, *20*, 466–478. [[CrossRef](#)]
29. Friston, K.J. The disconnection hypothesis. *Schizophr. Res.* **1998**, *30*, 115–125. [[CrossRef](#)]
30. Pearlson, G.D.; Marsh, L. Structural brain imaging in schizophrenia: A selective review. In *Biological Psychiatry*; Elsevier: Amsterdam, The Netherlands, 1999; Volume 46, pp. 627–649.
31. Calhoun, V.D.; Sui, J.; Kiehl, K.; Turner, J.; Allen, E.; Pearlson, G. Exploring the psychosis functional connectome: Aberrant intrinsic networks in schizophrenia and bipolar disorder. *Front. Psychiatry* **2012**, *2*, 75. [[CrossRef](#)] [[PubMed](#)]
32. Whitfield-Gabrieli, S.; Thermenos, H.W.; Milanovic, S.; Tsuang, M.T.; Faraone, S.V.; McCarley, R.W.; Shenton, M.E.; Green, A.I.; Nieto-Castanon, A.; LaViolette, P.; et al. Hyperactivity and hyperconnectivity of the default network in schizophrenia and in first-degree relatives of persons with schizophrenia. *Proc. Natl. Acad. Sci. USA* **2009**, *106*, 1279–1284. [[CrossRef](#)]
33. Salvador, R.; Sarró, S.; Gomar, J.J.; Ortiz-Gil, J.; Vila, F.; Capdevila, A.; Bullmore, E.; McKenna, P.J.; Pomarol-Clotet, E. Overall brain connectivity maps show cortico-subcortical abnormalities in schizophrenia. *Hum. Brain Mapp.* **2010**, *31*, 2003–2014. [[CrossRef](#)] [[PubMed](#)]
34. Fornito, A.; Zalesky, A.; Pantelis, C.; Bullmore, E.T. Schizophrenia, neuroimaging and connectomics. *Neuroimage* **2012**, *62*, 2296–2314. [[CrossRef](#)]
35. Ding, K.; Liu, Y.; Yan, X.; Lin, X.; Jiang, T. Altered functional connectivity of the primary visual cortex in subjects with amblyopia. *Neural Plast.* **2013**, *2013*, 612086. [[CrossRef](#)] [[PubMed](#)]
36. Li, S.; Li, P.; Gong, H.; Jiang, F.; Liu, D.; Cai, F.; Pei, C.; Zhou, F.; Zeng, X. Intrinsic functional connectivity alterations of the primary visual cortex in primary angle-closure glaucoma patients before and after surgery: A resting-State fMRI study. *PLoS ONE* **2017**, *12*, e0170598. [[CrossRef](#)] [[PubMed](#)]

37. Su, T.; Yuan, Q.; Liao, X.L.; Shi, W.Q.; Zhou, X.Z.; Lin, Q.; Min, Y.L.; Li, B.; Jiang, N.; Shao, Y. Altered intrinsic functional connectivity of the primary visual cortex in patients with retinal vein occlusion: A resting-state fMRI study. *Quant. Imaging Med. Surg.* **2020**, *10*, 958–969. [CrossRef] [PubMed]
38. Cohen, R.A. Cuneus. In *Encyclopedia of Clinical Neuropsychology*; Springer: New York, NY, USA, 2011; pp. 756–757.
39. Laycock, R.; Cross, A.J.; Lourenco, T.; Crewther, S.G. Dorsal stream involvement in recognition of objects with transient onset but not with ramped onset. *Behav. Brain Funct.* **2011**, *7*, 34. [CrossRef]
40. Parker, J.G.; Zalusky, E.J.; Kirbas, C. Functional MRI mapping of visual function and selective attention for performance assessment and presurgical planning using conjunctive visual search. *Brain Behav.* **2014**, *4*, 227–237. [CrossRef]
41. Noguchi, Y.; Inui, K.; Kakigi, R. Temporal dynamics of neural adaptation effect in the human visual ventral stream. *J. Neurosci.* **2004**, *24*, 6283–6290. [CrossRef] [PubMed]
42. Zeki, S. The disunity of consciousness. *Trends Cogn. Sci.* **2003**, *7*, 214–218. [CrossRef]
43. Haldane, M.; Cunningham, G.; Androustos, C.; Frangou, S. Structural brain correlates of response inhibition in Bipolar Disorder I. *J. Psychopharmacol.* **2008**, *22*, 138–143. [CrossRef] [PubMed]
44. Crockford, D.N.; Goodyear, B.; Edwards, J.; Quickfall, J.; El-Guebaly, N. Cue-induced brain activity in pathological gamblers. *Biol. Psychiatry* **2005**, *58*, 787–795. [CrossRef]
45. PDeweerd, P.; Iii, M.R.P.; DeSimone, R.; Ungerleider, L.G. Loss of attentional stimulus selection after extrastriate cortical lesions in macaques. *Nat. Neurosci.* **1999**, *2*, 753–758. [CrossRef] [PubMed]
46. Calhoun, V.D.; Adali, T.; Pearson, G.D.; Pekar, J.J. A method for making group inferences from functional MRI data using independent component analysis. *Hum. Brain Mapp.* **2001**, *14*, 140–151. [CrossRef]
47. Calhoun, V.D.; Liu, J.; Adali, T. A review of group ICA for fMRI data and ICA for joint inference of imaging, genetic, and ERP data. *Neuroimage* **2009**, *45*, S163–S172. [CrossRef]
48. Calhoun, V.D.; Adali, T. Multisubject independent component analysis of fMRI: A decade of intrinsic networks, default mode, and neurodiagnostic discovery. *IEEE Rev. Biomed. Eng.* **2012**, *5*, 60–73. [CrossRef]
49. Leonardi, N.; Richiardi, J.; Gschwind, M.; Simioni, S.; Annoni, J.M.; Schluep, M.; Vuilleumier, P.; Van De Ville, D. Principal components of functional connectivity: A new approach to study dynamic brain connectivity during rest. *Neuroimage* **2013**, *83*, 937–950. [CrossRef] [PubMed]
50. Allen, E.A.; Damaraju, E.; Plis, S.M.; Erhardt, E.B.; Eichele, T.; Calhoun, V.D. Tracking whole-brain connectivity dynamics in the resting state. *Cereb. Cortex* **2014**, *24*, 663–676. [CrossRef] [PubMed]
51. Cordes, D.; Haughton, V.; Carew, J.D.; Arfanakis, K.; Maravilla, K. Hierarchical clustering to measure connectivity in fMRI resting-state data. *Magn. Reson. Imaging* **2002**, *20*, 305–317. [CrossRef]
52. Li, X.; Zhu, D.; Jiang, X.; Jin, C.; Zhang, X.; Guo, L.; Zhang, J.; Hu, X.; Li, L.; Liu, T. Dynamic functional connectomics signatures for characterization and differentiation of PTSD patients. *Hum. Brain Mapp.* **2014**, *35*, 1761–1778. [CrossRef]
53. Lohmann, G.; Margulies, D.S.; Horstmann, A.; Pleger, B.; Lepsien, J.; Goldhahn, D.; Schloegl, H.; Stumvoll, M.; Villringer, A.; Turner, R. Eigenvector centrality mapping for analyzing connectivity patterns in fMRI data of the human brain. *PLoS ONE* **2010**, *5*, e10232. [CrossRef] [PubMed]
54. Norman, K.A.; Polyn, S.M.; Detre, G.J.; Haxby, J. V Beyond mind-reading: Multi-voxel pattern analysis of fMRI data. *Trends Cogn. Sci.* **2006**, *10*, 424–430. [CrossRef] [PubMed]
55. Zhu, F.; Kapitan, J.; Tranter, G.E.; Pudney, P.D.A.; Isaacs, N.W.; Hecht, L.; Barron, L.D. Residual structure in disordered peptides and unfolded proteins from multivariate analysis and ab initio simulation of Raman optical activity data. *Proteins Struct. Funct. Bioinform.* **2008**, *70*, 823–833. [CrossRef] [PubMed]
56. Achard, S.; Salvador, R.; Whitcher, B.; Suckling, J.; Bullmore, E. A resilient, low-frequency, small-world human brain functional network with highly connected association cortical hubs. *J. Neurosci.* **2006**, *26*, 63–72. [CrossRef] [PubMed]
57. Buckner, R.L.; Sepulcre, J.; Talukdar, T.; Krienen, F.M.; Liu, H.; Hedden, T.; Andrews-Hanna, J.R.; Sperling, R.A.; Johnson, K.A. Cortical hubs revealed by intrinsic functional connectivity: Mapping, assessment of stability, and relation to Alzheimer's disease. *J. Neurosci.* **2009**, *29*, 1860–1873. [CrossRef] [PubMed]
58. A Mini Review on Different Methods of Functional-MRI Data Analysis. Available online: <https://www.fortunejournals.com/articles/a-mini-review-on-different-methods-of-functional-mri-data-analysis.html> (accessed on 17 May 2021).
59. COBRE. Available online: http://fcon_1000.projects.nitrc.org/indi/retro/cobre.html (accessed on 29 October 2020).
60. Yan, C.G.; Wang, X.D.; Zuo, X.N.; Zang, Y.F. DPABI: Data Processing & Analysis for (Resting-State) Brain Imaging. *Neuroinformatics* **2016**, *14*, 339–351. [CrossRef]
61. SPM12 Software-Statistical Parametric Mapping. Available online: <https://www.fil.ion.ucl.ac.uk/spm/software/spm12/> (accessed on 29 September 2020).
62. MATLAB-MathWorks-MATLAB & Simulink. Available online: <https://www.mathworks.com/products/matlab.html> (accessed on 28 September 2020).
63. Friston, K.J.; Williams, S.; Howard, R.; Frackowiak, R.S.J.; Turner, R. Movement-related effects in fMRI time-series. *Magn. Reson. Med.* **1996**, *35*, 346–355. [CrossRef] [PubMed]
64. Ashburner, J. A fast diffeomorphic image registration algorithm. *Neuroimage* **2007**, *38*, 95–113. [CrossRef]
65. Biswal, B.B. Resting state fMRI: A personal history. *Neuroimage* **2012**, *62*, 938–944. [CrossRef]

66. He, C.; Chen, Y.; Jian, T.; Chen, H.; Guo, X.; Wang, J.; Wu, L.; Chen, H.; Duan, X. Dynamic functional connectivity analysis reveals decreased variability of the default-mode network in developing autistic brain. *Autism Res.* **2018**, *11*, 1479–1493. [[CrossRef](#)] [[PubMed](#)]
67. Xin, Q.; Ortiz-Terán, L.; Diez, I.; Perez, D.L.; Ginsburg, J.; El Fakhri, G.; Sepulcre, J. Sequence Alterations of Cortical Genes Linked to Individual Connectivity of the Human Brain. *Cereb. Cortex* **2018**, *29*, 3828–3835. [[CrossRef](#)]
68. Power, J.D.; Barnes, K.A.; Snyder, A.Z.; Schlaggar, B.L.; Petersen, S.E. Spurious but systematic correlations in functional connectivity MRI networks arise from subject motion. *Neuroimage* **2012**, *59*, 2142–2154. [[CrossRef](#)] [[PubMed](#)]
69. Tzourio-Mazoyer, N.; Landeau, B.; Papathanassiou, D.; Crivello, F.; Etard, O.; Delcroix, N.; Mazoyer, B.; Joliot, M. Automated anatomical labeling of activations in SPM using a macroscopic anatomical parcellation of the MNI MRI single-subject brain. *Neuroimage* **2002**, *15*, 273–289. [[CrossRef](#)]
70. Wang, K.; Liang, M.; Wang, L.; Tian, L.; Zhang, X.; Li, K.; Jiang, T. Altered functional connectivity in early Alzheimer's disease: A resting-state fMRI study. *Hum. Brain Mapp.* **2007**, *28*, 967–978. [[CrossRef](#)]
71. Preti, M.G.; Bolton, T.A.W.; Van De Ville, D. The dynamic functional connectome: State-of-the-art and perspectives. *Neuroimage* **2017**, *160*, 41–54. [[CrossRef](#)] [[PubMed](#)]
72. Shakil, S.; Lee, C.H.; Keilholz, S.D. Evaluation of sliding window correlation performance for characterizing dynamic functional connectivity and brain states. *Neuroimage* **2016**, *133*, 111–128. [[CrossRef](#)]
73. Li, Y.; Zhu, Y.; Nguchu, B.A.; Wang, Y.; Wang, H.; Qiu, B.; Wang, X. Dynamic Functional Connectivity Reveals Abnormal Variability and Hyper-connected Pattern in Autism Spectrum Disorder. *Autism Res.* **2020**, *13*, 230–243. [[CrossRef](#)] [[PubMed](#)]
74. Yu-Feng, Z.; Yong, H.; Chao-Zhe, Z.; Qing-Jiu, C.; Man-Qiu, S.; Meng, L.; Li-Xia, T.; Tian-Zi, J. Altered baseline brain activity in children with ADHD revealed by resting-state functional MRI. *Brain Dev.* **2007**, *29*, 83–91. [[CrossRef](#)]
75. Vidaurre, D.; Smith, S.M.; Woolrich, M.W. Brain network dynamics are hierarchically organized in time. *Proc. Natl. Acad. Sci. USA* **2017**, *114*, 12827–12832. [[CrossRef](#)]
76. Benjamini, Y.; Hochberg, Y. Controlling the False Discovery Rate: A Practical and Powerful Approach to Multiple Testing. *J. R. Stat. Soc. Ser. B Methodol.* **1995**, *57*, 289–300. [[CrossRef](#)]
77. Genovese, C.R.; Lazar, N.A.; Nichols, T. Thresholding of Statistical Maps in Functional Neuroimaging Using the False Discovery Rate. *Neuroimage* **2002**, *15*, 870–878. [[CrossRef](#)] [[PubMed](#)]
78. Wang, J.; Wang, X.; Xia, M.; Liao, X.; Evans, A.; He, Y. GREYNA: A graph theoretical network analysis toolbox for imaging connectomics. *Front. Hum. Neurosci.* **2015**, *9*, 386.
79. Aine, C.J.; Bockholt, H.J.; Bustillo, J.R.; Cañive, J.M.; Caprihan, A.; Gasparovic, C.; Hanlon, F.M.; Houck, J.M.; Jung, R.E.; Lauriello, J.; et al. Multimodal Neuroimaging in Schizophrenia: Description and Dissemination. *Neuroinformatics* **2017**, *15*, 343–364. [[CrossRef](#)] [[PubMed](#)]
80. Wang, L.; Alpert, K.I.; Calhoun, V.D.; Cobia, D.J.; Keator, D.B.; King, M.D.; Kogan, A.; Landis, D.; Tallis, M.; Turner, M.D.; et al. SchizConnect: Mediating neuroimaging databases on schizophrenia and related disorders for large-scale integration. *Neuroimage* **2016**, *124*, 1155–1167. [[CrossRef](#)] [[PubMed](#)]
81. Xiang, Y.; Wang, J.; Tan, G.; Wu, F.X.; Liu, J. Schizophrenia Identification Using Multi-View Graph Measures of Functional Brain Networks. *Front. Bioeng. Biotechnol.* **2020**, *7*, 479. [[CrossRef](#)]
82. Yang, B.; Chen, Y.; Shao, Q.-M.; Yu, R.; Li, W.-B.; Guo, G.-Q.; Jiang, J.-Q.; Pan, L. Schizophrenia Classification Using fMRI Data Based on a Multiple Feature Image Capsule Network Ensemble. *IEEE Access* **2019**, *7*, 109956–109968. [[CrossRef](#)]
83. Wang, H.L.S.; Rau, C.L.; Li, Y.M.; Chen, Y.P.; Yu, R. Disrupted thalamic resting-state functional networks in schizophrenia. *Front. Behav. Neurosci.* **2015**, *9*, 45. [[CrossRef](#)]
84. Yu, T.; Li, Y.; Fan, F.; Cao, H.; Luo, X.; Tan, S.; Yang, F.; Zhang, X.; Shugart, Y.Y.; Hong, L.E.; et al. Decreased Gray Matter Volume of Cuneus and Lingual Gyrus in Schizophrenia Patients with Tardive Dyskinesia is Associated with Abnormal Involuntary Movement. *Sci. Rep.* **2018**, *8*, 12884. [[CrossRef](#)] [[PubMed](#)]
85. Mané, A.; Falcon, C.; Mateos, J.J.; Fernandez-Egea, E.; Horga, G.; Lomeña, F.; Bargalló, N.; Prats-Galino, A.; Bernardo, M.; Parellada, E. Progressive gray matter changes in first episode schizophrenia: A 4-year longitudinal magnetic resonance study using VBM. *Schizophr. Res.* **2009**, *114*, 136–143. [[CrossRef](#)]
86. Zhou, P.; Wang, J.; Li, T.; Wang, N.; Xian, J.; He, H. Abnormal interhemispheric resting-state functional connectivity in primary open-angle glaucoma. In Proceedings of the 2016 38th Annual International Conference of the IEEE Engineering in Medicine and Biology Society (EMBC), Orlando, FL, USA, 16–20 August 2016; pp. 4055–4058. [[CrossRef](#)]
87. Ye, L.; Wei, R.; Huang, X.; Shi, W.Q.; Yang, Q.C.; Yuan, Q.; Zhu, P.W.; Jiang, N.; Li, B.; Zhou, Q.; et al. Reduction in interhemispheric functional connectivity in the dorsal visual pathway in unilateral acute open globe injury patients: A resting-state fMRI study. *Int. J. Ophthalmol.* **2018**, *11*, 1056–1060. [[CrossRef](#)] [[PubMed](#)]
88. Huang, X.; Li, D.; Li, H.J.; Zhong, Y.L.; Freeberg, S.; Bao, J.; Zeng, X.J.; Shao, Y. Abnormal regional spontaneous neural activity in visual pathway in retinal detachment patients: A resting-state functional MRI study. *Neuropsychiatr. Dis. Treat.* **2017**, *13*, 2849–2854. [[CrossRef](#)] [[PubMed](#)]
89. Giakoumatos, C.I.; Tandon, N.; Shah, J.; Mathew, I.T.; Brady, R.O.; Clementz, B.A.; Pearlson, G.D.; Thaker, G.K.; Tamminga, C.A.; Sweeney, J.A.; et al. Are structural brain abnormalities associated with suicidal behavior inpatients with psychotic disorders? *J. Psychiatr. Res.* **2013**, *47*, 1389–1395. [[CrossRef](#)] [[PubMed](#)]

90. Minzenberg, M.J.; Lesh, T.A.; Niendam, T.A.; Yoon, J.H.; Cheng, Y.; Rhoades, R.N.; Carter, C.S. Control-related frontal-striatal function is associated with past suicidal ideation and behavior in patients with recent-onset psychotic major mood disorders. *J. Affect. Disord.* **2015**, *188*, 202–209. [\[CrossRef\]](#)
91. Tohid, H.; Faizan, M.; Faizan, U. Alterations of the occipital lobe in schizophrenia. *Neurosciences* **2015**, *20*, 213–224. [\[CrossRef\]](#) [\[PubMed\]](#)
92. Tordesillas-Gutierrez, D.; Ayesa-Arriola, R.; Delgado-Alvarado, M.; Robinson, J.L.; Lopez-Morinigo, J.; Pujol, J.; Dominguez-Ballesteros, M.E.; David, A.S.; Crespo-Facorro, B. The right occipital lobe and poor insight in first-episode psychosis. *PLoS ONE* **2018**, *13*, e0197715. [\[CrossRef\]](#) [\[PubMed\]](#)
93. Glahn, D.C.; Laird, A.R.; Ellison-Wright, I.; Thelen, S.M.; Robinson, J.L.; Lancaster, J.L.; Bullmore, E.; Fox, P.T. Meta-Analysis of Gray Matter Anomalies in Schizophrenia: Application of Anatomic Likelihood Estimation and Network Analysis. *Biol. Psychiatry* **2008**, *64*, 774–781. [\[CrossRef\]](#) [\[PubMed\]](#)
94. Argyelan, M.; Ikuta, T.; Derosse, P.; Braga, R.J.; Burdick, K.E.; John, M.; Kingsley, P.B.; Malhotra, A.K.; Szeszko, P.R. Resting-state fMRI connectivity impairment in schizophrenia and bipolar disorder. *Schizophr. Bull.* **2014**, *40*, 100–110. [\[CrossRef\]](#) [\[PubMed\]](#)
95. Lynall, M.E.; Bassett, D.S.; Kerwin, R.; McKenna, P.J.; Kitzbichler, M.; Muller, U.; Bullmore, E. Functional connectivity and brain networks in schizophrenia. *J. Neurosci.* **2010**, *30*, 9477–9487. [\[CrossRef\]](#)
96. Phillips, O.R.; Nuechterlein, K.H.; Asarnow, R.F.; Clark, K.A.; Cabeen, R.; Yang, Y.; Woods, R.P.; Toga, A.W.; Narr, K.L. Mapping corticocortical structural integrity in schizophrenia and effects of genetic liability. *Biol. Psychiatry* **2011**, *70*, 680–689. [\[CrossRef\]](#)
97. Andreassen, N.C.; Flashman, L.; Flaum, M.; Arndt, S.; Swayze, V.; O'leary, D.S.; Ehrhardt, J.C.; Yuh, W.T.C. Regional Brain Abnormalities in Schizophrenia Measured With Magnetic Resonance Imaging. *JAMA* **1994**, *272*, 1763–1769. [\[CrossRef\]](#) [\[PubMed\]](#)
98. Bilder, R.M.; Wu, H.; Bogerts, B.; Degreef, G.; Ashtari, M.; Alvir, J.M.J.; Snyder, P.J.; Lieberman, J.A. Absence of regional hemispheric volume asymmetries in first-episode schizophrenia. *Am. J. Psychiatry* **1994**, *151*, 1437–1447. [\[CrossRef\]](#)
99. Bilder, R.M.; Wu, H.; Bogerts, B.; Ashtari, M.; Robinson, D.; Woerner, M.; Lieberman, J.A.; Degreef, G. Cerebral volume asymmetries in schizophrenia and mood disorders: A quantitative magnetic resonance imaging study. *Int. J. Psychophysiol.* **1999**, *34*, 197–205. [\[CrossRef\]](#)
100. Achim, A.M.; Lepage, M. Episodic memory-related activation in schizophrenia: Meta-analysis. *Br. J. Psychiatry* **2005**, *187*, 500–509. [\[CrossRef\]](#) [\[PubMed\]](#)
101. Fusar-Poli, P.; Perez, J.; Broome, M.; Borgwardt, S.; Placentino, A.; Caverzasi, E.; Cortesi, M.; Veggiotti, P.; Politi, P.; Barale, F.; et al. Neurofunctional correlates of vulnerability to psychosis: A systematic review and meta-analysis. *Neurosci. Biobehav. Rev.* **2007**, *31*, 465–484. [\[CrossRef\]](#)
102. Li, H.; Chan, R.C.K.; McAlonan, G.M.; Gong, Q.Y. Facial emotion processing in schizophrenia: A meta-analysis of functional neuroimaging data. *Schizophr. Bull.* **2010**, *36*, 1029–1039. [\[CrossRef\]](#) [\[PubMed\]](#)
103. Kottaram, A.; Johnston, L.; Ganella, E.; Pantelis, C.; Kotagiri, R.; Zalesky, A. Spatio-temporal dynamics of resting-state brain networks improve single-subject prediction of schizophrenia diagnosis. *Hum. Brain Mapp.* **2018**, *39*, 3663–3681. [\[CrossRef\]](#) [\[PubMed\]](#)
104. Fu, Z.; Iraj, A.; Turner, J.A.; Sui, J.; Miller, R.; Pearlson, G.D.; Calhoun, V.D. Dynamic state with covarying brain activity-connectivity: On the pathophysiology of schizophrenia. *Neuroimage* **2021**, *224*, 117385. [\[CrossRef\]](#) [\[PubMed\]](#)
105. Ma, S.; Calhoun, V.D.; Phlypo, R.; Adali, T. Dynamic changes of spatial functional network connectivity in healthy individuals and schizophrenia patients using independent vector analysis. *Neuroimage* **2014**, *90*, 196–206. [\[CrossRef\]](#)
106. Zhang, Y.; Guo, G.; Tian, Y. Increased Temporal Dynamics of Intrinsic Brain Activity in Sensory and Perceptual Network of Schizophrenia. *Front. Psychiatry* **2019**, *10*, 484. [\[CrossRef\]](#)
107. Bhinge, S.; Long, Q.; Calhoun, V.D.; Adali, T. Spatial Dynamic Functional Connectivity Analysis Identifies Distinctive Biomarkers in Schizophrenia. *Front. Neurosci.* **2019**, *13*, 1006. [\[CrossRef\]](#)
108. Nguyen, T.T.; Kovacevic, S.; Dev, S.I.; Lu, K.; Liu, T.T.; Eyler, L.T. Dynamic functional connectivity in bipolar disorder is associated with executive function and processing speed: A preliminary study. *Neuropsychology* **2017**, *31*, 73–83. [\[CrossRef\]](#)
109. Ding, Y.; Ou, Y.; Su, Q.; Pan, P.; Shan, X.; Chen, J.; Liu, F.; Zhang, Z.; Zhao, J.; Guo, W. Enhanced Global-Brain Functional Connectivity in the Left Superior Frontal Gyrus as a Possible Endophenotype for Schizophrenia. *Front. Neurosci.* **2019**, *13*, 145. [\[CrossRef\]](#)
110. Fusar-Poli, P.; Allen, P.; McGuire, P. Neuroimaging studies of the early stages of psychosis: A critical review. *Eur. Psychiatry* **2008**, *23*, 237–244. [\[CrossRef\]](#)
111. Kinney, D.K.; Matthyse, S. Genetic transmission of schizophrenia. *Annu. Rev. Med.* **1978**, *29*, 459–473. [\[CrossRef\]](#)
112. Zhang, S.; Li, C.S.R. Functional networks for cognitive control in a stop signal task: Independent component analysis. *Hum. Brain Mapp.* **2012**, *33*, 89–104. [\[CrossRef\]](#)
113. Bluhm, R.L.; Clark, C.R.; McFarlane, A.C.; Moores, K.A.; Shaw, M.E.; Lanius, R.A. Default network connectivity during a working memory task. *Hum. Brain Mapp.* **2011**, *32*, 1029–1035. [\[CrossRef\]](#)
114. Law, I.; Svarer, C.; Rostrup, E.; Paulson, O.B. Parieto-occipital cortex activation during self-generated eye movements in the dark. *Brain* **1998**, *121*, 2189–2200. [\[CrossRef\]](#)
115. Levy, D.L.; Holzman, P.S.; Matthyse, S.; Mendell, N.R. Eye tracking and schizophrenia: A selective review. *Schizophr. Bull.* **1994**, *20*, 47–62. [\[CrossRef\]](#)

-
116. Yang, E.; Tadin, D.; Glasser, D.M.; Hong, S.W.; Blake, R.; Park, S. Visual context processing in schizophrenia. *Clin. Psychol. Sci.* **2013**, *1*, 5–15. [[CrossRef](#)] [[PubMed](#)]
 117. Dakin, S.; Carlin, P.; Hemsley, D. Weak suppression of visual context in chronic schizophrenia. *Curr. Biol.* **2005**, *15*, R822–R824. [[CrossRef](#)]
 118. Meltzer, H.Y.; McGurk, S.R. The effects of clozapine, risperidone, and olanzapine on cognitive function in schizophrenia. *Schizophr. Bull.* **1999**, *25*, 233–255. [[CrossRef](#)]
 119. Sambataro, F.; Blasi, G.; Fazio, L.; Caforio, G.; Taurisano, P.; Romano, R.; Di Giorgio, A.; Gelao, B.; Bianco, L.L.; Papazacharias, A.; et al. Treatment with olanzapine is associated with modulation of the default mode network in patients with schizophrenia. *Neuropsychopharmacology* **2010**, *35*, 904–912. [[CrossRef](#)]
 120. Hindriks, R.; Adhikari, M.H.; Murayama, Y.; Ganzetti, M.; Mantini, D.; Logothetis, N.K.; Deco, G. Can sliding-window correlations reveal dynamic functional connectivity in resting-state fMRI? *Neuroimage* **2016**, *127*, 242–256. [[CrossRef](#)] [[PubMed](#)]
 121. Leonardi, N.; Van De Ville, D. On spurious and real fluctuations of dynamic functional connectivity during rest. *Neuroimage* **2015**, *104*, 430–436. [[CrossRef](#)]
 122. Mokhtari, F.; Akhlaghi, M.I.; Simpson, S.L.; Wu, G.; Laurienti, P.J. Sliding window correlation analysis: Modulating window shape for dynamic brain connectivity in resting state. *Neuroimage* **2019**, *189*, 655–666. [[CrossRef](#)]